e-ISSN: 2548-060X

International Journal of Energy Applications and Technologies

journal homepage: www.dergipark.gov.tr/ijeat

Original Research Article

The verify of experimentally drag reduction by flow control rod application on bus model using computational fluid dynamic

Cihan Bayindirli[1*], Mehmet Celik[2]

[1] *Nigde Vocational School of Technical Sciences, Nigde Omer Halisdemir University, Nigde, 51000, Türkiye*
[2] *Faculty of Engineering, Karabuk University, Karabük, 78100, Türkiye*

ARTICLE INFO

* Corresponding author
cbayindirli@ohu.edu.tr

Received December 7, 2021
Accepted December 23, 2021

Published by Editorial Board Members of IJEAT

doi: 10.31593/ijeat.1033791

ABSTRACT

Big percent of aerodynamic drag forces of road vehicles are pressure based. Therefore, it is important to examine the flow structure around the vehicles and take precautions against it. These studies are the subject of aerodynamics. Active and passive flow control are used to control the flow around the vehicle. In related studies, the use of CFD is a great advantage. In this study CFD method was used the verify of experimental drag reduction. The CFD tests were conducted at 6 different free flow velocities between the range of 3.8×10^3-7.9×10^3 Re. The model bus was drawn in SolidWorks after by 3D scanned. 10 mm, 20 mm and 30 mm diameter flow control rods were drawn and mounted at 3 different distance (L/H) to front surface of bus. CFD analyses were performed at the same test conditions for the least drag coefficient model. The experimental results were supported by CFD analyses in Fluent® program with 1.81% error margin. Detailed flow structures around the bus model and pressure distribution were determined by the CFD method.

Keywords: Aerodynamic; Road vehicle; Drag force; CFD; Passive flow control

1. Introduction

At the beginning of the 20th century, vehicle manufacturers prioritized producing fast vehicles. The fuel consumption and forces and of vehicles were not priority of them. But today they were focused on to aerodynamically designed road vehicles due to fuel prices and emissions limitation. The drag force effects to fuel consumption of vehicles especially high speeds. To achieve lower drag force and fuel consumption control of flow very important for vehicles. The flow separation can delay or prevent by flow control method and it effects both drag coefficient and vehicle performance values. Flow control methods were classified passive and active. The vehicle bodies have been modified in passive control technique. There is not any energy consume from the engine power in this technique [1,2]. Fuel consumption, emissions, noise problem are related to design and aerodynamic forces. When C_D coefficient decreased 2% fuel consumption can be reduced about 1% at high speeds [3-6]. In aerodynamic studies active and passive flow control techniques uses to flow control around of solid bodies. In passive flow control geometries has changed to get better aerodynamically shape. In that method there is not any energy spending. The biggest advantage of active method is this. [7-9]. Different flow control methods were researched and discussed in literature. In some papers two method were used together [10-12]. A lot of studies have been conducted not only getting the optimum aerodynamic design but also decrease fuel consumption. Aerodynamic drag forces of road vehicles increase with high speeds. 50% fuel consumption of road vehicles result from drag force [13-14]. Aerodynamic studies are very laborious and costly to work in real vehicle dimensions. In addition, errors in the outer body design of the vehicle after producing the vehicle increase the vehicle production process. So working with scale models in a wind tunnel is another method. Thanks to the recently developed

CFD software, the flow structure and aerodynamic forces around the vehicle can be calculated numerically. This provides great convenience to vehicle manufacturers and researchers. Computational Fluid Dynamics solve related flow equations. It is a numerical method for calculation for nonlinear differential equations describing/relating to fluid flow.

The purpose of this study is verify of experimental drag reduction by using flow control rod application in a study of Bayindirli, 2021 [15]. In related study 3 different diameter circular section flow control rod mounted on a bus model. Between the percent of 7.35%-10.06% drag reductions were obtained. In this study the model which has highest drag reduction was verified by CFD method. Besides detailed flow visualizations and distribution of total drag reduction were calculated. The original part of this study fuel consumption of a bus can decrease 5.5% by this pfc technique.

2. Material and Methods

In CFD tests 3 similarity conditions were provided. A licensed bus model was used to obtain drawing datas in 3D scanner. So geometric similarity was provided with that method. The sizes of solution domain were formed to obtain kinematic similarity. The blockage rate was 6.81% and it is acceptable in literature to provide kinematic similarity [16-17]. The Re is defined as the ratio of inertial forces to viscous forces as seen Eq.1.

$$R_e = \frac{U\infty L}{v} \tag{1}$$

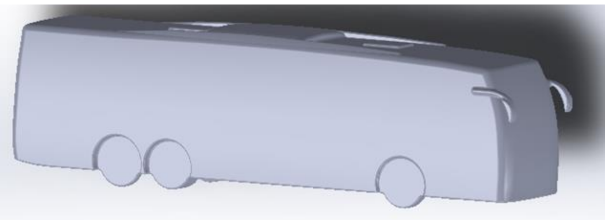

Fig. 1. The bus model in Solidworks [17]

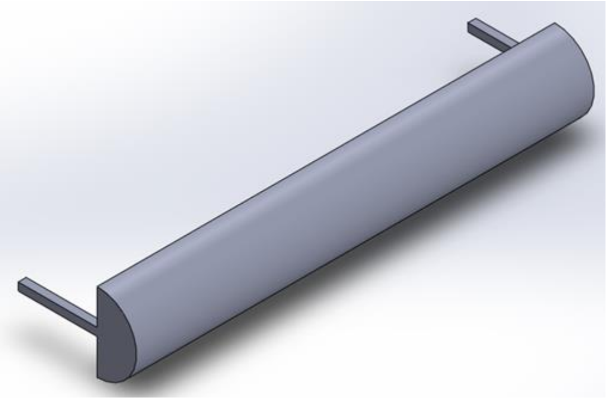

Figure 2. Solid Works drawing of a circular section flow control rod (D=10mm)

Re has to be same for model and prototype car in aerodynamic studies. But the size of prototype and model vehicle so different. Re independency uses to providing dynamic similarity in aerodynamic studies both wind tunnel and CFD. In this study Re independency was used to provide dynamic similarity. The CFD tests were conducted on the test model. It was given in Figure 1-2. The bus model is 1/33 scaled model of real size bus. The sizes of bus model are 101×96.3×441 mm [17].

2.1. Methodology in CFD

In CFD studies Fluent® package program was used to solve general integral equations. The program can solve related integral equations based on the finite volume method. The convergence value were used as 1.0×10^{-3} for x,y,z velocity and continuity. Turbulence intensity is 1%, air density 1 kg/m^3 and the dynamic viscosity 1.56x10^{-5} Ns/m^2. The frontal area of the bus model was determined as 0.0108 m^2. Flow analyses were made in standard initialization, standard wall functions and k-ε RNG turbulence model in a Workstation computer. Fluent® package software resolves related integral equations by using finite volume method. The mass balance in a volume was expressed a continuity equation (Eq.2). Accepting of density is constant provides important advantage in CFD flow analyses.

$$\frac{\partial \rho}{\partial t} + \frac{\partial(\rho u)}{\partial x} + \frac{\partial(\rho v)}{\partial y} + \frac{\partial(\rho w)}{\partial z} = 0 \tag{2}$$

$$\rho\left(\frac{\partial u}{\partial t} + u\frac{\partial u}{\partial x} + v\frac{\partial u}{\partial y} + w\frac{\partial u}{\partial z}\right) = -\frac{\partial p}{\partial x} + \rho g_x + \mu\left(\frac{\partial u^2}{\partial x^2} + \frac{\partial u^2}{\partial y^2} + \frac{\partial u^2}{\partial z^2}\right) \tag{3}$$

$$\rho\left(\frac{\partial v}{\partial t} + u\frac{\partial v}{\partial x} + v\frac{\partial v}{\partial y} + w\frac{\partial v}{\partial z}\right) = -\frac{\partial p}{\partial y} + \rho g_y + \mu\left(\frac{\partial v^2}{\partial x^2} + \frac{\partial v^2}{\partial y^2} + \frac{\partial v^2}{\partial z^2}\right) \tag{4}$$

$$\rho\left(\frac{\partial w}{\partial t} + u\frac{\partial w}{\partial x} + v\frac{\partial w}{\partial y} + w\frac{\partial w}{\partial z}\right) = -\frac{\partial p}{\partial z} + \rho g_z + \mu\left(\frac{\partial w^2}{\partial x^2} + \frac{\partial w^2}{\partial y^2} + \frac{\partial w^2}{\partial z^2}\right) \tag{5}$$

The solution domain was given in Figure 3. Dimensions of test section are 40x40x100 cm and it was generated in the same wind tunnel dimensions.

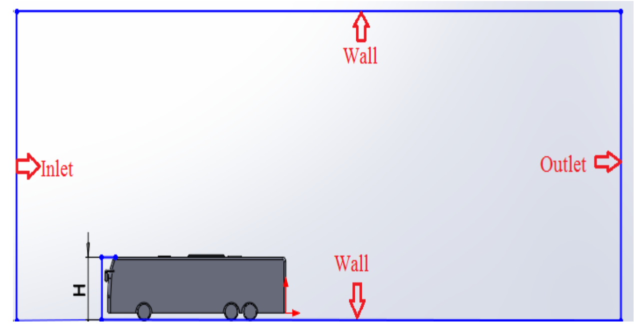

Fig. 3. The solution domain [5]

2.2. Mesh independency

At the beginning of numerical tests, the desired mesh distribution in solution domain were formed by changing the minimum and maximum element sizes. The mesh count was

1550251 in start as shown in Figure 4a, b. The adaptive meshing technique was used in tests in order to conduct with quality distribution of mesh. But still mesh independence tests were conducted to guarantee accuracy of CFD results. As seen in Table 1 independency tests were conducted on 10 different mesh distribution at 15 m/s free flow velocity.

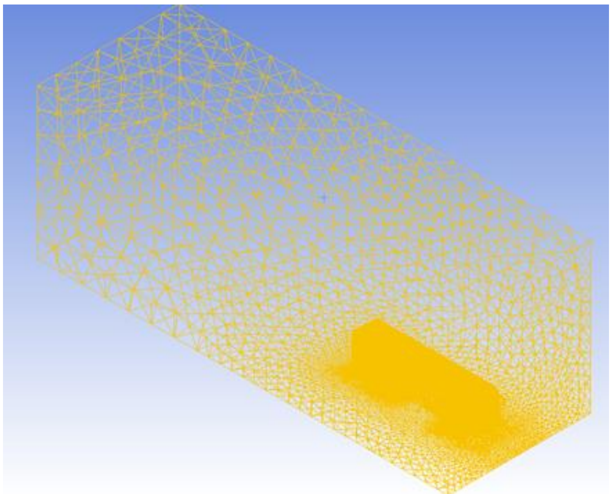

Fig. 4a. Mesh distribution in solution domain

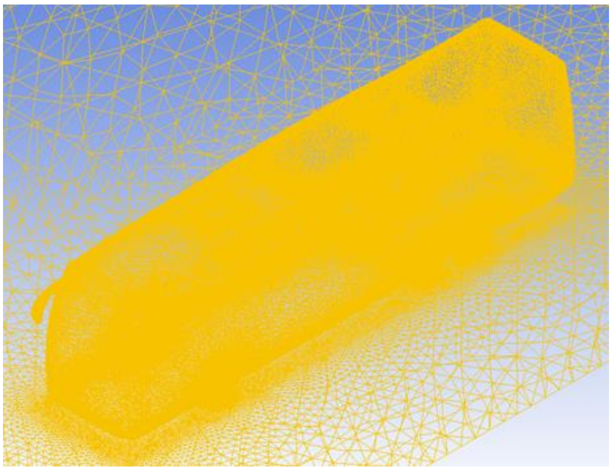

Fig. 4b. Mesh distribution on bus model

Table 1. Mesh independency test results at 5.4×10^3 Re

Re	Mesh Number	C_D
5.4×10^3	650306	0.56
5.4×10^3	954520	0.72
5.4×10^3	1060230	0.68
5.4×10^3	1550251	0.66
5.4×10^3	1995742	0.64
5.4×10^3	2227102	0.66
5.4×10^3	2602154	0.65
5.4×10^3	**2723079**	**0.65**
5.4×10^3	3565468	0.66
5.4×10^3	4011160	0.64

2.3. Adaptive meshing

2723079 tetrahedrons mesh were formed at the beginning. To provide high quality meshing adaptive grid mesh technique was used in tests. It is an effective method to obtain better mesh distribution and accuracy of numerical solutions in literature. The method enhances accuracy of analysis by cell enrichment or refinement, modifies the grid at regions where worse mesh distribution. In this technique, big mesh divide to small mesh and desired mesh distribution obtained. After first adaptive 3560131 mesh distribution was generated. Then refinements were applied in solution domain in each 100 iterations. After 6th adaptive, 8741128 mesh number were obtained and converged. The C_D was calculated based on Eq.6.

$$C_D = \frac{F_D}{\frac{1}{2}\rho V^2 A} \tag{6}$$

3. The Verify of Experimental Drag Reduction D=10 Mm, L/H=0.10)

The numerical results must verify or support with experimental tests in engineering studies as well as in studies about vehicle aerodynamics. Some researchers verify their results by comparing literature values. Verifying both results with another needs many effort and ability. The experimental test results were confirmed with CFD method in this study. Thus, the reliability of the study results was increased. The model which has maximum drag reduction was verified by CFD in same wind tunnel test conditions and same Re. Circular cross sectional shaped flow control rod drawn in diameter 10 mm and mounted on bus model L/H=0.1 distance. As result 11.16% numerically drag minimization was obtained in this model bus. It was 10.06% in wind tunnel tests [15]. Comparing wind tunnel-CFD results of best bus model were given in Table 2 and Figure 5-6. Flow images around of bus model were given in Figure 7-9.

Table 2. Comparing of experimental-numerical C_D values for best model and base model

Re	Best model CFD C_D	Base model CFD C_D	Best model Exp. C_D	Base model Exp. C_D
3.8×10^3	0.593	0.659	0.521	0.583
4.6×10^3	0.592	0.661	0.543	0.630
5.4×10^3	0.590	0.668	0.568	0.629
6.2×10^3	0.565	0.647	0.587	0.654
7.1×10^3	0.554	0.608	0.600	0.653
7.9×10^3	0.542	0.625	0.598	0.651
Average	**0.573**	**0.645**	**0.570**	**0.633**
Reduction	**11.16% in CFD**		**10.06% in wind tunnel**	

The much of pressure induced drag forms on the front bumper and windshield area of the bus. There are also stagnation pressures on the door mirrors and on the wheels as shown in Figure 8. The improvement of these areas should be a subject of another study.

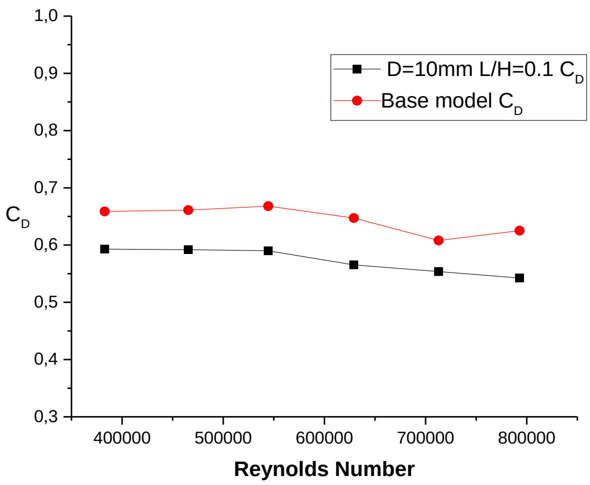

Fig. 5. Numerically drag minimization in model D=10mm L/H=0.1

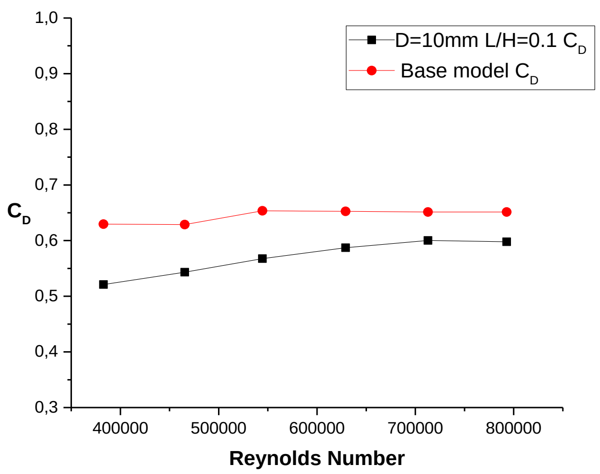

Fig. 6. Experimentally drag minimization in model D=10mm L/H=0.1

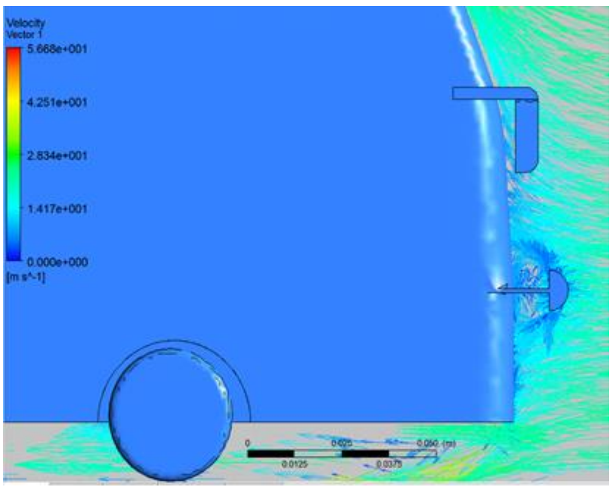

Figure 7. The vector visualization around of bus model at 7.9×105 Re

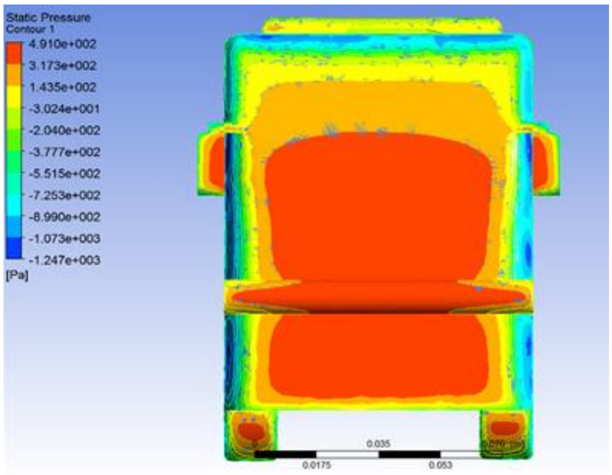

Fig. 8. The pressure distribution on bus model at 7.9×105 Re

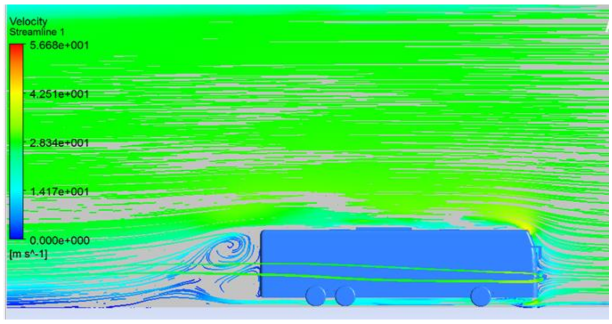

Fig. 9. The streamline visualization around of bus model at 7.9×105 Re

In this study a pfc method was used to decrease of pressure based drag force. By using this method the air flow brought out of ordinary flow. 10 mm diameter circular cross-sectional flow control rod positioned at 0.1 L/H distance on model bus. Aerodynamic drag force forms from friction and pressure based forces. In this study the desired drag reduction was obtained by decrease of pressure based drag force. As seen in flow visualizations there are very high pressure area on front of bus model. The stagnation pressure formed in application area. The air flow on the front bumper and windshield surface were redirected to the upper section of windshield surface by the circular cross-sectional control rod. Thus the pressure based aerodynamic was reduced by leaving the front surface region of the bus in the negative pressure area in the turbulent region. This situation explains that the source of the aerodynamic improvement result from this flow improvement in both studies.

4. Conclusions

In this paper the effect of circular cross-sectional control rod application to drag force was determined in Fluent. 10.06% experimentally drag reduction by using 10 mm diameters circular cross-sectional flow control rod was verified by CFD method. CFD analyses were carried out in the same test conditions. 11.16% drag minimization was obtained by CFD method. This result very close the experimental result and both experimental and numerical results support each other.

The achieved highest drag reduction was 11.16% after CFD tests. This reduction rate can be decreased fuel consumption by about 5.5% at high speeds (over 96 km/h). The total drag force forms from 89.07% pressure induced and 10.93% friction induced. It is determined that there is a big potential to decrease friction induced drag force for buses. It was numerically determined that the circular cross-sectional flow control rod application improved the flow structure around of bus.

ORCID

C. Bayindirli 0000-0001-9199-9670

M. Celik 0000-0002-3390-1716

A	**Frontal area of bus model, m^2**
C_D	Drag coefficient
F_D	Drag force, N
u_∞	Free stream velocity, m/s
Re	Re
ν	kinematic viscosity, m^2/s
ρ	Density of air, kg/m^3
CFD	Computational Fluid Dynamics
H	Height of model bus
L	Distance between model bus-spoiler
D	Diameter of flow control rod
V	Speed of vehicle km/h
LES	Large Eddy Simulation
RNG	Renormalization-Group
Exp.	Experimental
AFC	Active flow control
PFC	Passive flow control

References

[1] Cattafesta, L. N., and Sheplak, M. 2011. Actuators for active flow control. Annual Review of Fluid Mechanics, 43(1), 247-272.

[2] Altaf, A., Omar, A. Asrar. W. 2014. Review of passive drag reduction techniques for bluff road vehicles. IIUM Engineering Journal, 15(1), 61-69.

[3] Wood, R.M., and Bauer, S.X.S. 2003. Simple and low cost aerodynamic drag reduction devices for tractor-trailer Trucks. SAE Technical Paper, 01(3377), 1-18.

[4] Cui, W., Zhu, H., Xia. C. Yanga. Z. 2015. Comparison of steady blowing and synthetic jets for aerodynamic drag reduction of a simplified vehicle. Procedia Engineering, 126, 388-392.

[5] Bayındırlı. C., Akansu, Y.E. Celik, M. 2020. Experimental And Numerical Studies On Improvement Of Drag Force Of A Bus Model Using Different Spoiler Models. Int. J. Heavy Vehicle Systems, 27(6), 743-776.

[6] Hucho. W. H., and Sovran. G. 1993. Aerodynamics of road vehicles. Annual Review of Fluid Mechanics, 25(1), 485-537.

[7] Khalighi, B., Ho, J. Cooney, J. Neiswander, B. Corke, T. Han, T. 2016. Aerodynamic Drag Reduction Investigation for a Simplified Road Vehicle Using Plasma Flow Control. Proceedings of the ASME 2016 Fluids Engineering Division Summer Meeting.

[8] Tian, J., Zhang, Y. Zhu, H. Xiao, H. 2017. Aerodynamic drag reduction and flow control of Ahmed body with flaps. Advances in Mechanical Engineering, 9(7), 1-17.

[9] Bruneau, C.H., Creusé, E. Depeyras, D. Gilliéron, P. Mortazavi, I. 2010. Coupling active and passive techniques to control the flow past the square back Ahmed body. Computers & Fluids, 39,1875-1892.

[10] Mominul, I.M. and Mohammad, Z.A. 2019. Review on Aerodynamic Drag Reduction of Vehicles. International Journal of Engineering Materials and Manufacture, 4(1), 1-14.

[11] Yağız, B., Kandil, O. Pehlivanoglu, V.Y. 2012. Drag minimization using active and passive flow control technique. Aerospace Science and Technology, 17(1), 21–31.

[12] Sudin, M.N., Abdullah, M.A., Shamsuddin, S.A. Ramli, F.R. Tahir, M.M. 2014. Review of research on aerodynamic drag reduction method. International Journal of Mechanical and Mechatronics Engineering IJMME-IJENS, 14(2), 35-45.

[13] Mohamed, E.A., Radhwi, M.N. Abdel Gawad, A.F. 2015. Computational investigation of aerodynamic characteristics and drag reduction of a bus model. American Journal of Aerospace Engineering, 2(1-1), 64-73.

[14] Gillieron, P. and Kourta, A. 2013. Massive separation control analysis of the pulsed jet actuators effects. Mechanics & Industry, 14, 441-445.

[15] Bayindirli, C. 2021. Reducing of Pressure Based Drag Force of a Bus Model by Flow Control Rod in Wind Tunnel. International Journal of Automotive Science and Technology, 5(4), 412-418.

[16] Çengel. Y.A. Cimbala. J.M. 2008. Fluid Mechanics Fundamentals and Applications Güven Scientific Publications, 562-599.

[17] Bayindirli, C. Celik. M. 2018. The experimentally and numerically determination of the drag coefficient of a bus model. International Journal of Automotive Engineering and Technologies, 7(3), 117-123.